

# 2D DOA Estimation of UCA Correlative Interferometer Based on One Dimensional Sorting Lookup Table-Two Dimensional Linear Interpolation Algorithm

Kaibo CUI, Weiwei WU, Jingjian HUANG, Xi CHEN, Naichang YUAN

College of Electronic Science and Engineering, National University of Defense Technology, Changsha, Hunan, 410073, China

764608294@qq.com

Submitted December 26, 2016 / Accepted April 14, 2017

**Abstract.** *In order to improve the direction-finding efficiency of the correlative interferometer and reduce the size of the lookup table, this paper proposes the one dimensional sorting lookup table-two dimensional linear interpolation (1DSLUT-2DLI) algorithm. Firstly, the uniform circular array (UCA) model is established and the direction finding (DF) theory of the correlative interferometer is analyzed. A new lookup table is obtained by carrying out the ascending order for the first dimensional phase differences and a one dimensional iterative filtering method is used to look up the new table to get the direction of arrival (DOA) estimation. Compared to the exist methods, the 1DSLUT algorithm can reduce the computational complexity greatly. Considering the burden of a big lookup table, this paper proposes the 2DLI algorithm. Through the Taylor expansion, the conclusion that the phase difference is approximately linear in a small angle range is obtained. So, the linear interpolation can be applied to calculate the phase differences in the azimuth direction and elevation direction. On this basis, we conclude the equations to get the DOA estimation using the 2DLI algorithm. In this way, the size of the lookup table is reduced greatly, which decreases the computational complexity greatly also. The numerical simulations verify the effectiveness of the 1DSLUT-2DLI algorithm and it can obtain a pretty high DOA estimation precision with a low computational complexity and a small lookup table.*

## Keywords

UCA, correlative interferometer, 2D DOA estimation, direction-finding, 1DSLUT-2DLI algorithm

## 1. Introduction

Interferometer has the congenital advantage in the field of direction of arrival (DOA) estimation, such as high precision, simple structure and high sensitivity and so on. So, it has been widely used in radar, sonar and other detec-

tion equipment [1–4]. In order to acquire the high precision of direction finding, the traditional phase interferometers usually use the antenna array with long baseline. But when the baseline length exceeds the half wavelength of the incident signal, there will be the phase difference ambiguity problems for each array element [5], [6]. Although different authors proposed many methods to solve ambiguity [5–11], the success rate of solving ambiguity for a direction-finding system cannot be guaranteed because of the influence of array element structure, radome, element mutual coupling, etc. Especially in the case of high noise power, the ambiguity even cannot be solved. The correlative interferometer is a kind of interferometer direction finding system which uses the correlation techniques. The correlative interferometer breaks through the limitation that the antenna aperture must be less than half wavelength. And this interferometer avoids the problem of solving the phase ambiguity which exists in the phase interferometer. The direction-finding algorithm of the correlative interferometer is simple and it has been regarded as a high precision direction finding system by the International Telecommunication Union (ITU) [12]. So, it has been widely used in recent years [13–19]. As can be seen from the direction finding principal that the DOA estimation precision of the correlative interferometer must be ensured by the sample data precision, which inevitably brings about the high computational complexity and big data storage burden [12–16], [19]. Especially in the case of broadband signal and large view field, there will be impossible burdens for the processor. In order to solve this problem, a series of algorithms are proposed recently. In [17], the authors study a dimension separation-based two-dimensional correlation interferometer algorithm. The original two-dimensional angle searching is divided into 2 one-dimensional searching processes in the proposed algorithm to reduce the computational complexity. In [18], the authors propose a secondary correlation method of direction finding by using phase differences interpolation algorithm and the simulation results show that the algorithm has a much higher calculating speed while assuring good precision.

Because of the advantages of uniform circular array



$$\psi_{ij}^k = \frac{4\pi r f}{c} \sin \beta \sin \frac{k w}{2} \cdot \sin \left\{ \left[ j + N \left( \left\lfloor \frac{i+k}{N} \right\rfloor - 1 \right) - 1 - \frac{k}{2} \right] w + w_0 - \alpha \right\}, \quad (2)$$

$$i = 1, 2, \dots, N; k = 1, 2, \dots, K; j = i + k \setminus N.$$

In (2),  $r$  is the UCA radius,  $c$  is the speed of light,  $f$  is the frequency of the far-field signal.  $\setminus$  stands for taking remainders.  $\psi_{ij}^k$  is called the  $k$ th order and  $i$ th dimension phase difference of the UCA.

The following expressions can be obtained based on the geometric relationship in Fig. 1.

$$\begin{cases} \tan \alpha = \frac{\tan \theta}{\tan \varphi}, \\ \tan^2 \beta = \tan^2 \theta + \tan^2 \varphi. \end{cases} \quad (3)$$

Based on (2) and (3), the  $k$ th order and  $i$ th dimension phase difference of the UCA can be expressed as a function of azimuth angle and elevation angle, namely:

$$\begin{cases} \psi_{ij}^k = \frac{A_{ki} \tan \theta - B_{ki} \tan \varphi}{\sqrt{\tan^2 \theta + \tan^2 \varphi + 1}}, \\ A_{ki} = \frac{4\pi r f}{c} \sin \frac{k w}{2} \cdot \sin \left\{ \left[ j + N \left( \left\lfloor \frac{i+k}{N} \right\rfloor - 1 \right) - 1 - \frac{k}{2} \right] w + w_0 \right\}, \\ B_{ki} = \frac{4\pi r f}{c} \sin \frac{k w}{2} \cdot \cos \left\{ \left[ j + N \left( \left\lfloor \frac{i+k}{N} \right\rfloor - 1 \right) - 1 - \frac{k}{2} \right] w + w_0 \right\}, \\ i = 1, 2, \dots, N; k = 1, 2, \dots, K; j = i + k \setminus N. \end{cases} \quad (4)$$

### 3. The 1DSLUT-2DLI Algorithm

#### 3.1 The Analysis of UCA Correlative Interferometer

As can be seen from (4) that we can get the  $k$ th order and  $i$ th dimension phase difference of the UCA based on the azimuth angle and elevation angle of incident wave. In turn, the procedure of estimating DOAs of the incident signals through the phase differences is called the interferometer direction finding. The correlative interferometer is a kind of direction finding system which obtains the DOA of signals through the correlation between the phase difference of incident wave and the phase difference sample data. The overall thought of direction finding methods for the correlative interferometer can be expressed as the follows. Firstly, the phase differences of the array elements can be obtained by looping through the whole field of the

correlative interferometer and these phase differences can be regarded as the sample data to form the lookup table, which regards the azimuth angle and the elevation angle as the index. Then, the phase differences of the real incident signal can be compared with the phase differences stored in the lookup table and the highest correlation point can be selected. Finally, the DOA estimation can be obtained from the index of the highest correlation point. Assuming the phase difference stored in the lookup table is  $\psi^k(\theta, \varphi)$  and the phase difference of the incident wave is  $\tilde{\psi}^k$ . The direction-finding process is to find the highest correlation point between  $\tilde{\psi}^k$  and  $\psi^k(\theta, \varphi)$  to get  $(\theta, \varphi)$  of the point, which can be expressed as the following expression.

$$(\theta, \varphi) = f(\tilde{\psi}^k, \psi^k(\theta, \varphi)). \quad (5)$$

In (5),  $f(\cdot)$  is the phase difference comparison function. As the phase difference value is from  $-\pi$  to  $\pi$ , so there is a flip phenomenon for the phase difference at  $\pm\pi$ , which will cause a bigger direction finding error. In order to solve this problem, in this paper, we use the maximum cosine sum criterion [13], [14] as the comparison function, which can be expressed as follows.

$$f(\tilde{\psi}^k, \psi^k(\theta, \varphi)) = \max_{(\theta, \varphi)} \left( \sum_{i=1}^N \cos(\tilde{\psi}_{ij}^k - \psi_{ij}^k(\theta, \varphi)) \right). \quad (6)$$

For a UCA interferometer, the main factors which influence its direction-finding precision are the element number, the array radius, the phase difference order and the incident wave frequency. As the correlative interferometer uses the looking up table algorithm, so it avoids the problem of solving the phase ambiguity. In [20], the authors propose that UCA is non-oriented fuzzy when the number of the elements is an odd number greater than 5 or an even number greater than 8. So we just analyze the direction finding precision of the UCA correlative interferometer. According to (4), the derivatives of  $\psi_{ij}^k$  with azimuth angle and elevation angle can be obtained, namely:

$$\frac{d\psi_{ij}^k}{d\theta} = \frac{B_{ki} \tan \theta \tan \varphi + A_{ki} \tan^2 \varphi + A_{ki}}{\cos^2 \theta (\tan^2 \theta + \tan^2 \varphi + 1)^{3/2}}, \quad (7)$$

$$\frac{d\psi_{ij}^k}{d\varphi} = \frac{A_{ki} \tan \theta \tan \varphi - B_{ki} \tan^2 \varphi - B_{ki}}{\cos^2 \varphi (\tan^2 \theta + \tan^2 \varphi + 1)^{3/2}}. \quad (8)$$

Based on the definition of derivative, when  $\Delta\psi_{ij}^k \rightarrow 0$ , the following expressions can be obtained.

$$\Delta\theta = \frac{\cos^2 \theta (\tan^2 \theta + \tan^2 \varphi + 1)^{3/2}}{B_{ki} \tan \theta \tan \varphi + A_{ki} \tan^2 \varphi + A_{ki}} \Delta\psi_{ij}^k, \quad (9)$$

$$\Delta\varphi = \frac{\cos^2 \theta (\tan^2 \theta + \tan^2 \varphi + 1)^{3/2}}{A_{ki} \tan \theta \tan \varphi - B_{ki} \tan^2 \varphi - B_{ki}} \Delta\psi_{ij}^k. \quad (10)$$

As can be seen from (9) and (10) that when the incident wave direction is determined, the values of  $\Delta\theta$  and  $\Delta\varphi$  can be calculated by  $A_{ki}$  and  $B_{ki}$ . Based on (4), we can get

the following conclusions. The larger the radius of UCA, the smaller  $\Delta\theta$  and  $\Delta\varphi$ , which means the higher the DOA estimation precision. The larger the element number, the higher the DOA estimation precision. The higher the frequency of the incident wave, the higher the DOA estimation precision. The higher the phase difference order, the higher the DOA estimation precision.

Through the theory analysis of the correlative interferometer, we can see that when the UCA parameters and the incident wave parameters are determined, the direction-finding precision is determined by the step angle of the lookup table. The smaller the step angle is, the higher the direction-finding precision. When we estimate the DOA based on (6), we need to calculate every point of the lookup table. So, the smaller the step angle is, the higher the computational complexity of the algorithm. Especially in the case of two-dimensional direction finding, the computational complexity will increase in square times with the decrease of the step angle. In addition, the smaller the step angle is, the bigger the size of the lookup table, which will bring about the impossible storing burdens for the processor.

### 3.2 The 1DSLUT Algorithm

According to (1), we can see that for the phase differences of UCA, when the UCA parameters and the incident wave parameters are determined, it is determined by the incident wave direction. So, each dimension of the  $k$ th order phase difference sample data in the lookup table is corresponding to each dimension of the  $k$ th order phase difference of the incident wave. So, we can contrast each dimension of the  $k$ th order phase difference one by one and pick out the highest correlation point. Considering the phase differences between the lookup table and the incident wave are different because of the noises, so the maximum cosine sum criterion can be expressed as the following expression, which is the one-dimensional lookup table algorithm.

$$f(\tilde{\psi}^k, \psi^k(\theta, \varphi)) = \begin{cases} (\theta_1, \varphi_1) = \cos(\tilde{\psi}_{1j}^k - \psi_{1j}^k(\theta, \varphi)) > T_1 \\ (\theta_m, \varphi_m) = \cos(\tilde{\psi}_{mj}^k - \psi_{mj}^k(\theta_{m-1}, \varphi_{m-1})) > T_m \\ (\theta_N, \varphi_N) = \max_{(\theta_{N-1}, \varphi_{N-1})} \cos(\tilde{\psi}_{1j}^k - \psi_{1j}^k(\theta_{N-1}, \varphi_{N-1})) \\ k = 1, 2, \dots, N; m = 2, \dots, N-1; j = m+k \setminus N. \end{cases} \quad (11)$$

As can be seen from (11), the one-dimensional lookup table algorithm is a kind of iteration comparison method. In (11),  $m$  expresses the  $m$ th comparison of the algorithm and  $T_m$  is the comparison threshold of the  $m$ th comparison which is determined by the noise level.  $(\theta_m, \varphi_m)$  is a collection of the points within the comparison threshold after the  $m$ th comparison. We can see from (11) that the number of points within the threshold after each comparison is less and less. So the algorithm can improve the calculation efficiency. It is important to note that if there is only one

point in  $(\theta_m, \varphi_m)$  after the  $m$ th comparison, this point is the DOA estimation of the incident wave. If there is no point in  $(\theta_m, \varphi_m)$  after the  $m$ th comparison, we can obtain the DOA estimation of the incident wave by solving the expression:  $(\theta_m, \varphi_m) = \max_{(\theta_{m-1}, \varphi_{m-1})} \cos(\tilde{\psi}_{mj}^k - \psi_{mj}^k(\theta_{m-1}, \varphi_{m-1}))$ .

Otherwise, we can obtain the DOA estimation  $(\theta_N, \varphi_N)$  based on (11), which will carry out  $N$  iteration comparisons.

As can be seen from the theory of the 1DLUT algorithm,  $T_m$  is the main factor of this algorithm.  $T_m$  is a positive number less than 1, which represents the proximity between the phase differences of the incident wave and the phase differences stored in the lookup table. If  $T_m$  is set too big, the correct DOA information will probably be got rid of after some iteration. If  $T_m$  is set too little, the number of the points within the comparison threshold after some iteration will be relatively big, which will bring about the increase of the computational complexity. In addition, if  $T_m$  is set too little, the effect of the random noises will be increased, which will cause a wrong estimation. Generally speaking, the deviation caused by the random noises for each dimension of the  $k$ th order phase difference belongs to a same range, so we select a same comparison threshold for each iteration, namely:

$$T_m = T_1 = T, m = 2, \dots, N-1. \quad (12)$$

As can be seen from (11) that when we carry out the first iteration, we need to carry out the threshold comparison for the first dimensional phase differences of all the points in the view filed. In order to further decrease the computational complexity of the algorithm, we can sort the phase difference sample values in an ascending order firstly and the angle information will be stored in the lookup table in the meantime. Then, we can take the points whose phase difference of the first dimension owns a difference with the first dimensional phase differences in the lookup table less than  $\pm\Delta\xi$  as the results of the first iteration. We sort the phase difference sample values when we establish the lookup table, which will not increase the computational complexity of the algorithm. In this way, we can avoid carrying out the threshold comparison for the first dimensional phase differences of all the points in the view filed, which can decrease the computational complexity of the algorithm greatly.  $\Delta\xi$  can be obtained from  $T$ , namely:

$$\Delta\xi = \arccos(T). \quad (13)$$

Compared to the conventional algorithm in [13], the 1DSLUT algorithm decreases the number of points which need to be calculated and the size of the lookup table remains the same. The number of points which need to be calculated is shown in Fig. 2.

In Fig. 2, the solid line stands for the conventional algorithm and the dotted line represents the 1DSLUT algorithm. In addition, the solid line also represents the size of the lookup table. As can be seen from the figure, for the conventional algorithm in [13], the number of points need

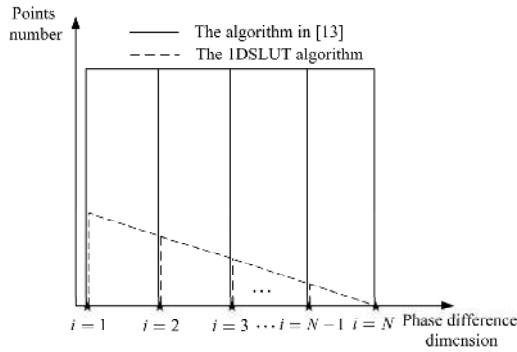


Fig. 2. The points' number to be calculated.

to be calculated is the number of points stored in the lookup table. However, for the 1DSLUT algorithm, the number of points need to be calculated decreases along with the increase of the phase difference dimension and the number of points is also far less than the number of points of the traditional algorithm. So, the 1DSLUT algorithm can greatly decrease the computational complexity compared to the traditional algorithm.

### 3.3 The 2DLI Algorithm

As can be seen from the analysis in Sec. 3.2, no matter we choose the conventional algorithm or the 1DSLUT algorithm, the size of the lookup table is not changed, so the direction-finding precision is also determined by the step angle of the lookup table. However, there is an irreconcilable conflict between the step angle and the computational complexity. If we want to get a DOA estimation result with high precision, the step angle of the lookup table must be little, which will cause that the size of the lookup table is very big. So, it is difficult to store the table and the real-time performance of the algorithm also cannot be guaranteed. In order to control the size of the lookup table, this paper proposes the 2DLI algorithm.

Firstly, we can get the Taylor expansions of  $\psi_{ij}^k$  in (4) at  $\theta = 0$  and  $\varphi = 0$  separately.

$$\psi_{ij}^k(\theta, \varphi) = \frac{B_{ki} \tan \varphi}{(\tan^2 \varphi + 1)^{1/2}} + \frac{A_{ki}}{(\tan^2 \varphi + 1)^{1/2}} \theta + \frac{B_{ki} \tan \varphi}{2(\tan^2 \varphi + 1)^{5/2}} \theta^2 + o(\theta), \quad (14)$$

$$\psi_{ij}^k(\theta, \varphi) = \frac{A_{ki} \tan \theta}{(\tan^2 \theta + 1)^{1/2}} - \frac{B_{ki}}{(\tan^2 \theta + 1)^{1/2}} \varphi - \frac{A_{ki} \tan \theta}{2(\tan^2 \theta + 1)^{5/2}} \varphi^2 + o(\varphi). \quad (15)$$

In (14) and (15),  $o(\theta)$  and  $o(\varphi)$  are the high-order terms of  $\psi_{ij}^k(\theta, \varphi)$ . As can be seen from (14) and (15), the coefficient of the high-order terms of  $\psi_{ij}^k(\theta, \varphi)$  are smaller and smaller. So, when  $\varphi$  is a certain value,  $\psi_{ij}^k(\theta, \varphi)$  can be regarded as a linear function in a small range of  $\theta$ . In the same way, when  $\theta$  is a certain value,  $\psi_{ij}^k(\theta, \varphi)$  can be regarded as a linear function in a small range of  $\varphi$ . Based on this, we

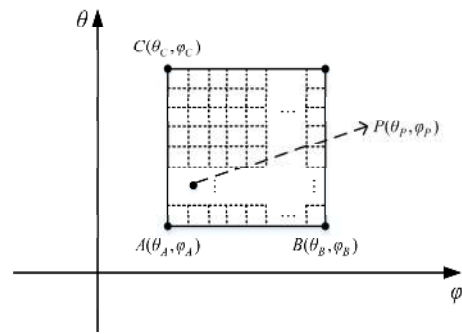


Fig. 3. The sketch map of the two-dimensional interpolation.

can carry out the linear interpolation for phase differences in the azimuth direction and elevation direction. The interpolation can be explained by Fig. 3.

In Fig. 3, the lookup table is expressed as a two-dimensional plane in the rectangular coordinate system.  $A(\theta_A, \varphi_A)$ ,  $B(\theta_B, \varphi_B)$  and  $C(\theta_C, \varphi_C)$  are the adjacent points in the lookup table. Assuming the DOA of the incident wave is located at  $P(\theta_P, \varphi_P)$ . The phase difference of the  $k$ th order and the  $i$ th dimension is  $\psi_{ij}^k(\theta_P, \varphi_P)$ . We can see from Fig. 3 that the point which is most close to  $P$  is  $A$ , which means the direction-finding result is  $(\theta_A, \varphi_A)$  when using the conventional algorithm. The phase difference of the  $k$ th order and the  $i$ th dimension of  $A$  is  $\psi_{ij}^k(\theta_A, \varphi_A)$ . The next adjacent point of  $A$  in the azimuth direction is  $B$ , whose phase difference of the  $k$ th order and the  $i$ th dimension is  $\psi_{ij}^k(\theta_B, \varphi_B)$ . The next adjacent point of  $A$  in the elevation direction is  $C$ , whose phase difference of the  $k$ th order and the  $i$ th dimension is  $\psi_{ij}^k(\theta_C, \varphi_C)$ . If the step angle of the lookup table in the azimuth direction is  $\tau_\theta$  and the step angle in the elevation direction is  $\tau_\varphi$ , we can get the following expressions.

$$\begin{cases} (\theta_B, \varphi_B) = (\theta_A, \varphi_A + \tau_\varphi), \\ (\theta_C, \varphi_C) = (\theta_A + \tau_\theta, \varphi_A). \end{cases} \quad (16)$$

The result of looking up the table with no interpolation is  $(\theta_A, \varphi_A)$ . The two-dimensional linear interpolation is to carry out the linear interpolation in the azimuth direction and the elevation direction for the phase differences in the original lookup table, which is expressed as the dotted lines in Fig. 3. To put it simply, the interpolation is to make the rectangle composed by  $A$ ,  $B$  and  $C$  more dense, so that we can get the point which is more close to  $P$ . If the interpolation multiple in the azimuth direction and elevation direction are separately  $L_\theta$  and  $L_\varphi$ , we can get the position of  $P$  in the two dimensional interpolation plane.

$$\theta_P = \theta_A + \frac{1}{N} \sum_{i=1}^N \frac{\psi_{ij}^k(\theta_P, \varphi_P) - \psi_{ij}^k(\theta_A, \varphi_A)}{\psi_{ij}^k(\theta_C, \varphi_C) - \psi_{ij}^k(\theta_A, \varphi_A)} L_\theta \cdot \frac{\tau_\theta}{L_\theta}, \quad (17)$$

$$\varphi_P = \varphi_A + \frac{1}{N} \sum_{i=1}^N \frac{\psi_{ij}^k(\theta_P, \varphi_P) - \psi_{ij}^k(\theta_A, \varphi_A)}{\psi_{ij}^k(\theta_B, \varphi_B) - \psi_{ij}^k(\theta_A, \varphi_A)} L_\varphi \cdot \frac{\tau_\varphi}{L_\varphi}. \quad (18)$$

In (17) and (18), in order to decrease the influence of the random noises, we carry out the linear interpolation for the  $k$ th order phase differences of  $N$  dimensions and regard

the mean value as the final result. In this way, we can improve the direction-finding precision of the correlative interferometer on the basis that the size of the lookup table remains unchanged.

### 4. Numerical Simulation

In order to test the performance of the proposed algorithm, we carry out the numerical simulation. The UCA correlative interferometer parameters are shown in Tab. 1.

Firstly, we can get the sample data of phase differences by looping through the whole view field and establish the lookup table. The phase differences of the incident wave can be obtained by overlaying phase differences of the lookup table and the random noises, namely:

$$\tilde{\psi}^k = \psi^k + \sigma^2 . \tag{19}$$

In (19),  $\sigma^2$  represents the power of the random noises.

#### 4.1 The 1DSLUT Algorithm

We can obtain the new lookup table based on the method described in Sec. 3.2. Firstly, we simulate the relationship between  $T$  and the algorithm performance. The parameters of the UCA correlative interferometer are shown in Tab. 1. The frequency of the incident wave is 5 GHz. We carry out a total of 1000 times Monte Carlo simulations for the whole view field and count the direction-finding error probability. The results are shown in Fig. 4.

In Fig. 4, the error probability is the percentage of the error direction finding points in the whole view field. When the measuring errors of angles are bigger than the step angle of the lookup table, we consider it to be an error direction finding point. As can be seen from the figure, under the various noise power, the error probability increases sharply with the increase of  $T$  after  $T > 0.95$ . This is because the correct DOA information is got rid of. When  $T < 0.95$ , under the low noise power situation (5 dBm, 10 dBm), the error probability increases a little (less than 0.03) with the increase of  $T$ , which can be ignored. Under the high noise power (15 dBm, 20 dBm), the error probability presents a parabola form, which means the error probability decreases with the increase of  $T$  firstly and then increases with the increase of  $T$ . The change range is huge

Sensor number	7	The array radius [m]	0.18
$w_0$	$3\pi / 14$	$w$	$2\pi / 7$
Azimuth field [°]	(-45,45)	Pitch field [°]	(-45,45)
The azimuth stepping angle [°]	1	The pitch stepping angle [°]	1
$k$	1		

Tab. 1. The parameters of the UCA correlative interferometer.

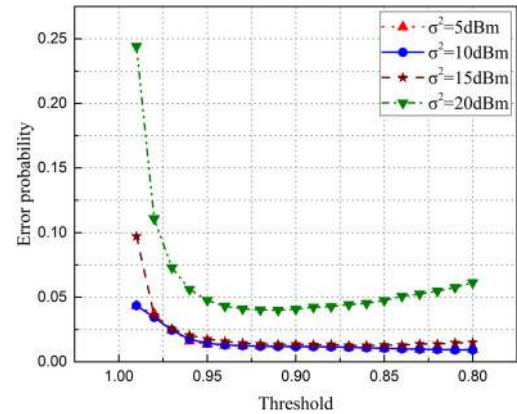


Fig. 4. The relationship between  $T$  and the error probability.

in the case of high noise power (even more than 0.2 when  $\sigma^2$  is 20 dBm). When  $T = 0.90\sim 0.95$ , the error probability is lower. According to the theory of the 1DSLUT algorithm, the higher the threshold is, the higher the computational complexity. In order to concern both the efficiency and the accuracy, we pick up  $T = 0.94$  in this paper. Based on (13), we can obtain  $\Delta\xi \approx 20^\circ$ .

In order to further examine the performance of the 1DSLUT algorithm, we carry out the comparison simulation between the conventional algorithm in [13] and the 1DSLUT algorithm. The simulation parameters remain unchanged. We carry out a total of 1000 times Monte Carlo simulations and the results are shown in Fig. 5.

In Fig. 5, we show the relationship between the noise power and the direction-finding error probability of the two algorithms. As can be seen from the figure, the error probability of the algorithm in [13] is somewhat less than the error probability of the 1DSLUT algorithm. However, the difference of the error probability between the two algorithms is very small (less than 0.03), so the 1DSLUT algorithm can meet the practical requirements.

For the 1DSLUT algorithm, it has the advantage of lower computational complexity. So, we count the number of points which need to be calculated in these two algorithms. For the lookup table in Tab. 1, the data points' number is 8281. So, the number of points which need to be

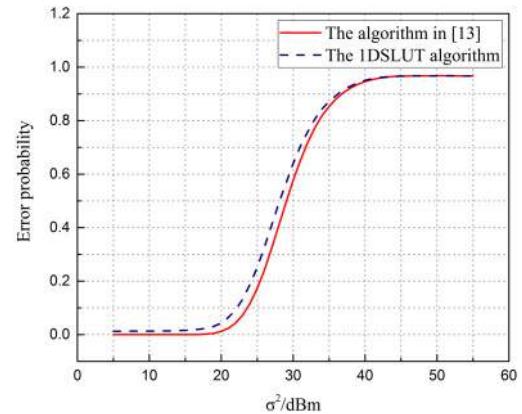


Fig. 5. The relationship between  $\sigma^2$  and the error probability of the two algorithms.

	The data points
The first iteration	990
The second iteration	877
The third iteration	197
The fourth iteration	116
The fifth iteration	23
The sixth iteration	14

Tab. 2. The points' number within the threshold after each iteration for the 1DSLUT algorithm.

	The algorithm in [13]	The 1DSLUT algorithm
Addition	49686	0
Subtraction	57967	2217
Cosine	57967	2217
Comparison	8281	2217

Tab. 3. The times of all kinds of operation for the two algorithms.

calculated in the conventional algorithm is 8281. For the 1DSLUT algorithm, we count the points' number within the threshold after each iteration which are shown in Tab. 2.

In Tab. 2, the points' number after each iteration is the points' number needed to be calculated for the next iteration. As the first iteration is carried out through getting a series of points in the lookup table directly, so we omit it. The results in Tab. 2 are the mean values of all the incident waves in the view field. As can be seen from the table, the points' number after each iteration decreases rapidly, which is matched with the theory analysis in Sec. 3.2.

In the simulation, if we use the algorithm in [13], based on (6), we need to carry out 7 times subtraction operation, 7 times cosine operation, 6 times addition operation and 1 time comparison operation at each point. If we use the 1DSLUT algorithm, based on (11), we need to carry out 1 times subtraction operation, 1 time cosine operation and 1 time comparison operation at each point. Based on the above analysis, we can obtain the times of all kinds of operation for the two algorithms when they carry out one time direction finding. The results are shown in Tab. 3.

As can be seen from the results in Tab. 3, the times of all the operations for the 1DSLUT algorithm decrease more than 30 times compared to the algorithm in [13]. So, the 1DSLUT algorithm has a huge advantage in terms of the computational complexity.

## 4.2 The 2DLI Algorithm

In order to examine the performance of the 2DLI algorithm proposed in Sec. 3.3, we carry out the numerical simulations. The parameters of the correlative interferometer are shown in Tab. 1. The interpolation multiple in the azimuth direction and elevation direction are all 100. In order to fully inspect the performance of the two-dimensional interpolation, we set 5 incident wave signals. The signals are assigned the number 1~5 and their frequencies are all 5 GHz. The two dimensional DOA respectively are

$(-40^\circ, -15^\circ)$ ,  $(-20^\circ, 40^\circ)$ ,  $(10^\circ, -35^\circ)$ ,  $(30^\circ, 5^\circ)$ , and  $(0^\circ, 0^\circ)$ , which means they distribute in four quadrants and the origin.

Figure 6 shows the interpolation errors of the five signals, which can be obtained by the subtraction between the phase differences after interpolation and the phase differences in the lookup table whose step angle is  $0.01^\circ$ . In addition, the interpolation errors in Fig. 6 are the sum of the azimuth interpolation errors and the elevation interpolation errors. As can be seen from the figure, for the signals from different directions, the interpolation errors are different. The interpolation errors are related to the distance between the signal directions and the origin. The farther the distance, the smaller the interpolation error. But the interpolation errors of different signals are all pretty small (less than  $0.05^\circ$ ), which won't have effects on the direction finding basically.

In order to further examine the performance of the 2DLI algorithm, we also analyze the relationship between the DOA estimation precision of the above five signals and the power of noises. The DOA estimation precision can be measured by the root mean square error (RMSE). As this paper carries out a 2-D DOA estimation, the RMSE is a combination between the azimuth angle estimation error and the elevation angle estimation error, namely:

$$RMSE = \sqrt{\frac{1}{num} \sum_{j=1}^{num} (\tilde{\theta}_j - \theta)^2 + (\tilde{\varphi}_j - \varphi)^2}. \quad (20)$$

In (20),  $num$  stands for the number of the Monte Carlo simulation.  $\tilde{\theta}_j$  is the azimuth angle estimation of the  $j$ th simulation and  $\tilde{\varphi}_j$  is the elevation angle estimation of the  $j$ th simulation.

In addition to a decreasing noise power, the other parameters remain unchanged. We carry out a total of 1000 times Monte Carlo simulations and the results are shown in Fig. 7.

As can be seen from Fig. 7, when  $\sigma^2$  is 20 dBm, the RMSE of DOA estimations of different signals is less than  $1.4^\circ$ , so the 2DLI algorithm owns a pretty high precision for the DOA estimation. The RMSE of DOA estimations

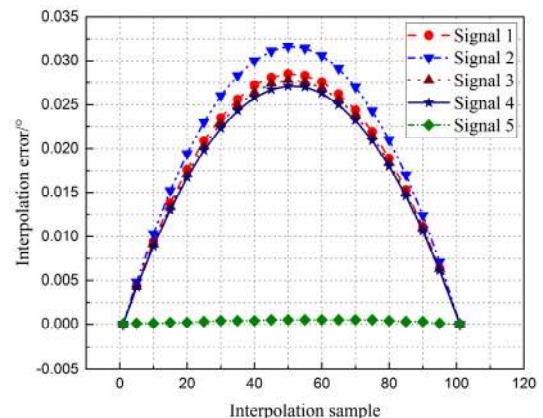


Fig. 6. The interpolation errors of the five signals.

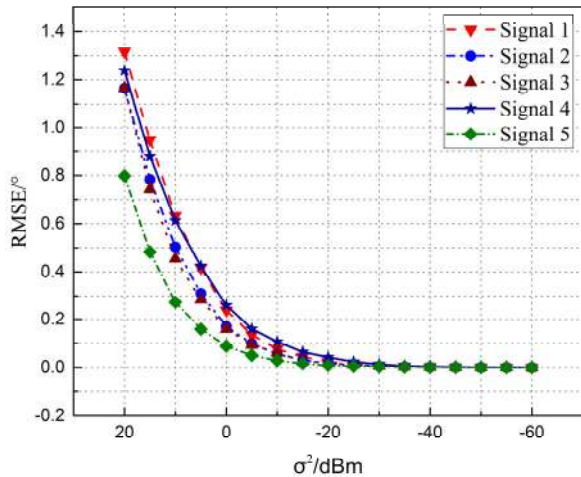


Fig. 7. RMSE of DOA estimation along with the noises' power.

decreases rapidly with the decrease of the noises' power and achieves the convergence condition (The RMSE is infinitely close to zero) ultimately. For a UCA interferometer, it has isotropy for the waves of different directions in theory, but the DOA estimation precision for the waves from different directions are not the same in Fig. 7. This is because of the random errors when establishing the lookup table and the random noises when imitating the incident wave signals. We also can see from Fig. 7 that there is no clear correlation between the RMSE of DOA estimations and the interpolation errors shown in Fig. 6. This is because the interpolation errors are pretty small and the noises are the main factor which influences the DOA estimation precision.

### 4.3 The 1DSLUT-2DLI Algorithm

As can be seen from the derivation in Sec. 3.1, for a UCA correlative interferometer, the main factors which influence its direction-finding precision are the element number, the array radius, the phase difference order and the incident wave frequency. In order to examine the performance of the 1DSLUT-2DLI algorithm, we also simulate the relationship between these factors and the DOA estimation precision. The parameters of the UCA correlative interferometer are shown in Tab. 1. The incident wave signal is from  $(-4^\circ, 9^\circ)$  whose frequency is 5 GHz. We carry out a total of 1000 times Monte Carlo simulations and the results are shown in Fig. 8.

Figure 8(a) shows the DOA estimation RMSE along with the noises' power using three different phase difference orders. As can be seen from the figure, in all situations, the estimation RMSE decreases with the decrease of the noises' power and achieves the convergence condition ultimately. In addition, the higher the phase difference order, the lower the DOA estimation RMSE. Figure 8(b) shows the DOA estimation RMSE along with the array radius in four different noises' power. As can be seen from the figure, the estimation RMSE decreases with the increase of the array radius and the higher the noises' power,

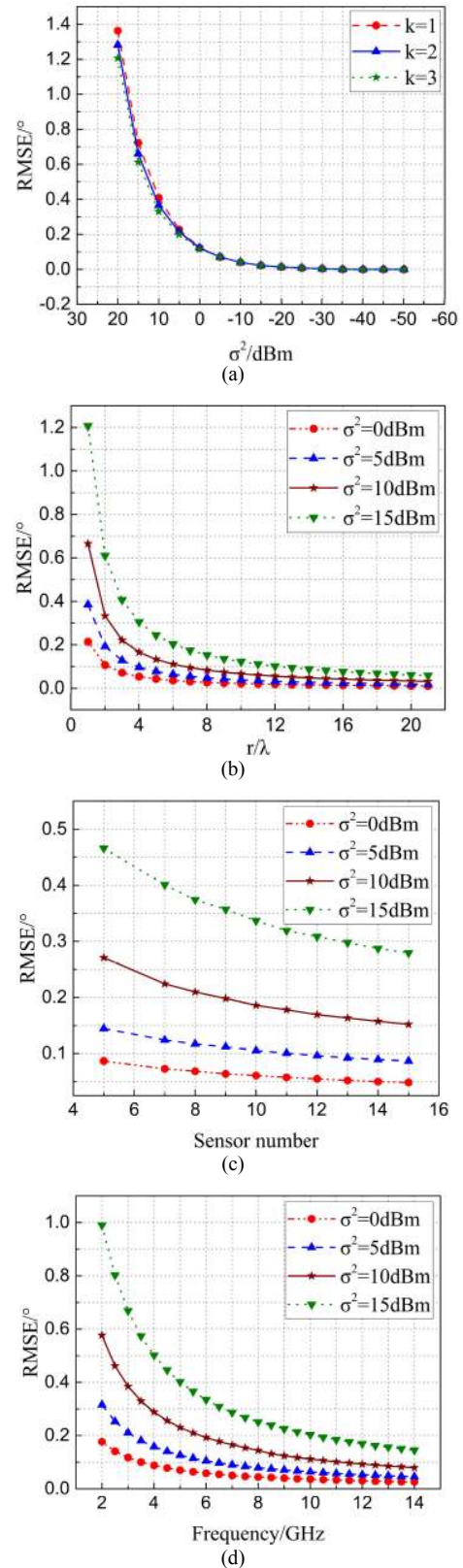


Fig. 8. The relationship between the DOA estimation precision and the various factors when using the 1DSLUT-2DLI algorithm. (a) is the relationship between RMSE and the phase difference order. (b) is the relationship between RMSE and the radius of the array. (c) is the relationship between RMSE and the sensor number. (d) is the relationship between RMSE and the sensor number.



the bigger the decrement of the estimation RMSE with the increase of the array radius. Figure 8(c) shows the DOA estimation RMSE along with the sensor number in four different noises' power. In order to carry out the direction finding with no ambiguity, we get rid of the UCA with 6 elements [20]. As can be seen from the figure, the estimation RMSE decreases with the increase of the sensor number and the higher the noises' power, the bigger the decrement of the estimation RMSE with the increase of the sensor number. Figure 8(d) shows the DOA estimation RMSE along with the frequency of the signal in four different noises' power. As can be seen from the figure, the estimation RMSE decreases with the increase of the signal frequency and the higher the noises' power, the bigger the decrement of the estimation RMSE with the increase of the signal frequency. The simulation results shown in Fig. 8 are matched with the theory analysis in Sec. 3.1. In addition, we can see from the simulation results that the 1DSLUT-2DLI algorithm shows a pretty good estimation precision in various cases.

#### 4.4 Algorithm Comparison

In order to further examine the performance of the proposed algorithm, we carry out a comparison simulation using a series of algorithms, which are:

- Algorithm 1: the 1DSLUT-2DLI algorithm. The step angle of the lookup table is  $1^\circ$  and the interpolation multiple is 100.
- Algorithm 2: the algorithm in [13]. The step angle of the lookup table is  $1^\circ$ . Algorithm 2 uses the maximum cosine sum criterion [13].
- Algorithm 3: the algorithm in [13]. The step angle of the lookup table is  $0.01^\circ$ . Algorithm 3 uses the maximum cosine sum criterion [13].
- Algorithm 4: the algorithm in [17]. The step angle of the lookup table is  $1^\circ$  and the interpolation multiple is 100. Algorithm 4 uses the maximum correlation coefficient criterion [13], [14] in the azimuth direction and the maximum cosine sum criterion in the elevation direction [17].
- Algorithm 5: the algorithm in [18]. The step angle of the original lookup table is  $1^\circ$  and the interpolation multiple is 100. Algorithm 5 uses the maximum correlation coefficient criterion [18].

The frequency of the incident signal is 5 GHz and its DOA is  $(8.37^\circ, -9.73^\circ)$ . The other parameters except for the lookup table are shown in Tab. 1. We carry out a total of 1000 times Monte Carlo simulations and the results are shown in Fig. 9.

Figure 9 shows the estimation RMSE along with the noises' power using five different algorithms. As can be seen from the results, when using these five algorithms, the RMSE of DOA estimation all decreases rapidly with the decrease of the noises' power and achieves the conver-

gence condition ultimately. However, when using Algorithm 2, the estimation RMSE can't converge to zero or a number infinitely close to zero. This is because the step angle of the lookup table in Algorithm 2 is too big, which causes the estimation precision is low. For the rest of algorithms, the RMSE all can converge to zero or a number infinitely close to zero. Among them, Algorithm 3 is using a pretty small step angle of the lookup table, which can improve the DOA estimation greatly. Algorithm 1, Algorithm 4 and Algorithm 5 all make use of the same lookup table compared to Algorithm 2. However, these three algorithms all take advantage of the interpolation, which can improve the estimation precision on the basis of remaining the lookup table unchanged.

In terms of the DOA estimation precision, except for different lookup tables, Algorithm 2 and Algorithm 3 use the same algorithm proposed in [13], so we just analyze the estimation precision of Algorithm 1, Algorithm 3, Algorithm 4 and Algorithm 5. In general, Algorithm 3 owns the highest estimation precision, followed by Algorithm 1, Algorithm 4 and Algorithm 5. As can be seen from Fig. 9, the estimation precision of the 1DSLUT-2DLI algorithm is improved a lot compared to the Algorithm 4 and Algorithm 5. Especially in the case of high noise's power, the precision improvement is very obvious. When  $\sigma^2$  is 20 dBm, the RMSE is reduced more than  $0.11^\circ$  compared to Algorithm 4 and more than  $0.23^\circ$  compared to Algorithm 5. Although the estimation accuracy of Algorithm 3 is better than the proposed algorithm, the superiority is not big. When  $\sigma^2$  is 20 dBm, the RMSE of Algorithm 3 is reduced only about  $0.03^\circ$  compared to the proposed algorithm. With the decrease of the noises' power, the estimation RMSE of these four algorithms tend to be the same (When  $\sigma^2$  is 0 dBm, the four RMSE curves are basically coincident), which means the DOA estimation precision of four algorithms tends to be the same.

Although Algorithm 3 owns the highest estimation precision in these five algorithms, its lookup table's size is 10000 times compared to the lookup table's size of other algorithms. Considering the simulation results in Sec. 4.1,

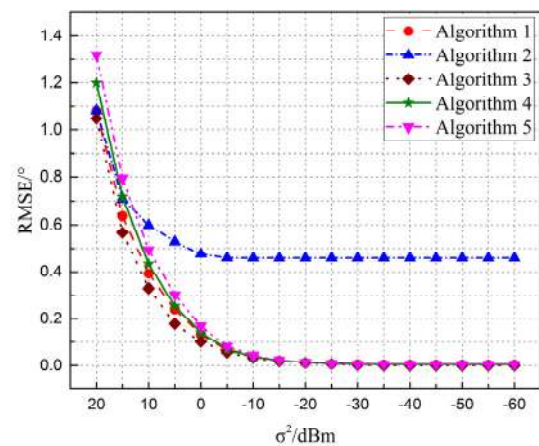


Fig. 9. RMSE of DOA estimation along with the noises' power using five different algorithms.

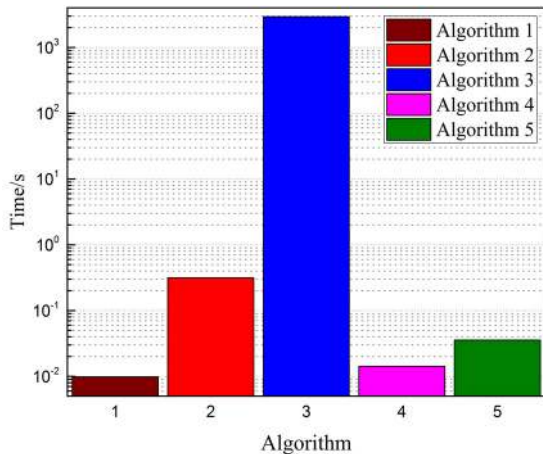


Fig. 10. The estimation time of these five algorithms when running on Matlab.

we can conclude that in order to obtain a similar estimation precision, the computational complexity decreases more than 300 000 ( $30 \times 10\ 000$ ) times when using the proposed algorithm instead of Algorithm 3. For Algorithm 2 and Algorithm 5, the lookup table's size is equal, however, the computational complexity of the maximum cosine sum criterion is somewhat smaller than that of the maximum correlation coefficient criterion, so the computational complexity of Algorithm 2 is smaller than that of Algorithm 5. According to the simulation results in Sec. 4.1, we can conclude that the computational complexity decreases more than 30 times when using the proposed algorithm instead of Algorithm 2 and Algorithm 5. For Algorithm 4, its data points' number needed to be calculated is smaller than that of Algorithm 1, however, its various operation times is bigger than that of Algorithm 1, so the computational complexity of Algorithm 4 is comparative to the computational complexity of the proposed algorithm. However, Algorithm 4 and Algorithm 5 all need to solve the phase ambiguity, which increases the computational complexity. In addition, the success rate of solving ambiguity cannot be guaranteed because of the influence of array element structure, radome, element mutual coupling, etc. Especially in the case of high noises' power, the ambiguity even cannot be solved, which limits the application of these two algorithms.

In order to further compare the computation complexity, the direction finding efficiencies of these five algorithms are compared. In the computer platform with an Intel Core i7-2600K CPU @3.40GHz, we choose Matlab as a programming language to investigate the average time of carrying out 1000 runs. The results are shown in Fig. 10.

As can be seen from the figure, Algorithm 1 needs the lowest direction finding time, followed by Algorithm 4, Algorithm 5, Algorithm 2 and Algorithm 3. So, Algorithm 1 offers the highest direction finding efficiency, which means it owns the lowest computational complexity. The results shown in Fig. 10 are in accordance with the previous analysis and simulations for these five algorithms.

## 5. Conclusion

In order to improve the direction-finding efficiency of correlative interferometer and reduce the size of the lookup table, this paper proposes the 1DSLUT-2DLI algorithm. The algorithm can be applied to a UCA correlative interferometer and can complete the non-ambiguity 2D DOA estimation of the far-field incident wave with a high precision. The proposed algorithm also does not need to solve the phase ambiguity, which makes it can be used in various complex environments. The numerical simulation results verify the effectiveness of the 1DSLUT-2DLI algorithm, which can obtain a pretty high DOA estimation precision with a low computational complexity and a small lookup table. So, it is prone to be realized in engineering.

## References

- [1] PAN, Y. J., ZHANG, X. F., XIE, S. Y., et al. An ultra-fast DOA estimator with circular array interferometer using lookup table method. *Radioengineering*, 2015, vol. 24, no. 3, p. 850–856. DOI: 10.13164/re.2015.0850
- [2] LIU, Z. M., GUO, F. C. Azimuth and elevation estimation with rotating long-baseline interferometers. *IEEE Transactions on Signal Processing*, 2015, vol. 63, no. 9, p. 2405–2419. DOI: 10.1109/TSP.2015.2405506
- [3] ZHANG, M., GUO, F. C., ZHOU, Y. Y. A closed-form solution for moving source localization using LBI changing rate of phase difference only. *Chinese Journal of Aeronautics*, 2014, vol. 27, no. 2, p. 365–374. DOI: 10.1016/j.cja.2014.02.013
- [4] NANZER, A. J. Sensitivity of a passive correlation interferometer to an angularly moving source. *IEEE Transactions on Microwave Theory and Techniques*, 2012, vol. 60, no. 12, p. 3868–3876. DOI: 10.1109/TMTT.2012.2217982
- [5] JACOBS, E., RALSTON, E. W. Ambiguity resolution in interferometry. *IEEE Transactions on Aerospace and Electronic Systems*, 1981, vol. 17, no. 6, p. 766–780. DOI: 10.1109/TAES.1981.309127
- [6] PACE, P. E., WICKERSHAM, D., JENN, D. C., et al. High-resolution phase sampled interferometry using symmetrical number systems. *IEEE Transactions on Antennas and Propagation*, 2001, vol. 49, no. 10, p. 1411–1423. DOI: 10.1109/8.954930
- [7] SUNDARAM, K. R., MALLIK, R. K., MURTHY, U. M. S. Modulo conversion method for estimating the direction of arrival. *IEEE Transactions on Aerospace and Electronics Systems*, 2000, vol. 36, no. 4, p. 1391–1396. DOI: 10.1109/7.892687
- [8] QU, Z. Y., SI, S. C. Direction finding method of wideband passive radar seeker based on virtual baseline. *Journal of Projectiles, Rockets, Missiles and Guidance*, 2007, vol. 27, no. 4, p. 92–95. DOI: 10.3969/j.issn.1673-9728.2007.04.028 (in Chinese)
- [9] SI, W. J., CHU, P., SUN, S. H. Research on solving ambiguity technology based on semi-circle array. *Systems Engineering and Electronics*, 2008, vol. 30, no. 11, p. 2128–2131. DOI: 10.3321/j.issn:1001-506X.2008.11.023 (in Chinese)
- [10] CUI, X. Phase interferometer improvement based on virtual baseline. *Communications Technology*, 2011, vol. 44, no. 7, p. 89–91. DOI: 10.3969/j.issn.1002-0802.2011.07.033 (in Chinese)

- [11] ZHANG, C. J., LI, Z. D. Research on solving ambiguity error of nonuniform circular antenna array model. *Systems Engineering and Electronics*, 2012, vol. 34, no. 8, p. 1525–1529. DOI: 10.3969/j.issn.1001-506X.2012.08.01 (in Chinese)
- [12] WANG, C. H. Correlation interferometer and its application. *China Radio Management*, 2001, vol. 8, p. 28–29. DOI: 10.3969/j.issn.1672-7797.2001.08.013 (in Chinese)
- [13] PARK, C. S., KIM, D. Y. The fast correlative interferometer direction finder using I/Q demodulator. In *2006 Asia-Pacific Conference on Communications (APCC 2006)*. 2006. 5 p. DOI: 10.1109/APCC.2006.255915
- [14] WEI, H. W., SHI, Y. G. Performance analysis and comparison of correlative interferometers for direction finding. In *IEEE 10<sup>th</sup> International Conference on Signal Processing (ICOSP)*. Beijing (China), 2010, p. 393–396. DOI: 10.1109/ICOSP.2010.5657185
- [15] HAN, G., WANG, B., CHEN, J. Y. Researching on algorithm suitable for implementation of correlation interferometer direction finding with FPGA. *Computer Engineering and Design*, 2010, vol. 31, no. 20, p. 4365–4367. (in Chinese)
- [16] QIAN, Z. B., CHEN, N. Fast implementation of correlation interferometer direction finding based on DSP. *Radio Engineering of China*, 2011, vol. 41, no. 8, p. 47–50. DOI: 10.3969/j.issn.1003-3106.2011.08.016 (in Chinese)
- [17] CHENG, T., GUI, X. T., ZHANG, X. A dimension separation-based two-dimensional correlation interferometer algorithm. *EURASIP Journal on Wireless Communications and Networking*, 2013, vol. 2013, no. 1, p. 1–10. DOI: 10.1186/1687-1499-2013-40
- [18] XIE, S. G., HAO, X. C., ZENG, X. Y., et al. A secondary correlation method of direction finding based on phase differences interpolation algorithm. *Chinese Journal of Radio Science*, 2014, vol. 29, no. 1, p. 183–187. DOI: 10.13443/j.cjors.2013032301 (in Chinese)
- [19] LIM, J. S., CHAE, G. S. Analysis of direction finding accuracy for amplitude-phase comparison and correlative interferometer method. *Journal of Digital Convergence*, 2016, vol. 14, no. 1, p. 195–201. DOI: 10.14400/JDC.2016.14.1.195
- [20] XIAO, W., XIAO, X. C., TAI, H. M. Rank-1 ambiguity DOA estimation of circular array with fewer sensors. In *Proceedings of the 45th IEEE Midwest Symposium on Circuits and Systems (MWSCAS-2002)*. Tulsa (USA), 2002, p. III-29–III-32. DOI: 10.1109/MWSCAS.2002.1186962
- [21] WANG, P., LI, Y. H., VUCETIC, B. Millimeter wave communications with symmetric uniform circular antenna arrays. *IEEE Communications Letters*, 2014, vol. 18, no. 8, p. 1307–1310. DOI: 10.1109/LCOMM.2014.2332334
- [22] DORSEY, W. M., COLEMAN, J. O., PICKLES, W. R. Uniform circular array pattern synthesis using second-order cone programming. *IET Microwaves, Antennas & Propagation*, 2015, vol. 9, no. 8, p. 723–727. DOI: 10.1049/iet-map.2014.0418
- [23] JACKSON, B. R., RAJAN, S., LIAO, B. J., et al. Direction of arrival estimation using directive antennas in uniform circular arrays. *IEEE Transactions on Antennas and Propagation*, 2015, vol. 63, no. 2, p. 736–747. DOI: 10.1109/TAP.20142384044
- [24] WANG, M., MA, X. C., YAN, S. F., et al. An autocalibration algorithm for uniform circular array with unknown mutual coupling. *IEEE Antennas and Wireless Propagation Letters*, 2016, vol. 15, p. 12–15. DOI: 10.1109/LAWP.2015.2425423

## About the Authors ...

**Kaibo CUI** was born in 1990. He received his M.S. degree in Electronic Science and Technology from the National University of Defense Technology in 2013. Currently he is working towards the Ph.D. degree in the College of Electronic Science and Engineering, National University of Defense Technology, Changsha, Hunan, China. His research interests include signal processing and spatial spectrum estimation.

**Weimei WU** was born in 1981. She received her M.S. and Ph.D. degree in Electronic Science and Technology from the National University of Defense Technology in 2008 and 2011, respectively. Currently she is a teacher in the College of Electronic Science and Engineering, National University of Defense Technology, Changsha, Hunan, China. Her research interests include array signal processing and antenna design.

**Jingjian HUANG** was born in 1983. He received his Ph.D. degree in Electronic Science and Technology from the National University of Defense Technology in 2014. Currently he is a teacher in the College of Electronic Science and Engineering, National University of Defense Technology, Changsha, Hunan, China. His research interests include antenna design.

**Xi CHEN** was born in 1983. He received his Ph.D. degree in Electronic Science and Technology from the National University of Defense Technology in 2013. Currently he is a teacher in the College of Electronic Science and Engineering, National University of Defense Technology, Changsha, Hunan, China. His research interests include signal processing.

**Naichang YUAN** was born in 1965. He received his M.S. and Ph.D. degree in Electronic Science and Technology from the University Science and Technology of China in 1991 and 1994, respectively. He is currently a professor with the College of Electronic Science and Engineering, National University of Defense Technology, Changsha, Hunan, China. His research interests include array signal processing, signal processing in radar.